

Preliminary qualitative analysis of Metabolites

All the solvent-based extracts were subjected to preliminary qualitative phytochemical screening. The results indicate that alkaloids, saponins, tannins, flavonoids, phenols, and phytosterols were found to be higher in methanolic extract compared to other extracts. Anthraquinone and coumarins were absent in all the extracts Table S1.

Table S1. Qualitative analysis of *Kalanchoe laciniata*.

S.No	Compounds	Fresh Powder
1.	Carbohydrates	++
2.	Protein	+
3.	Saponin	+++
4.	Phenolics	+++
5.	Flavonoids	+
6.	Alkaloids	+
7.	Tannins	+
8.	Phytosterols	+
9.	Glycosides	+
10.	Amino Acids	+++
11.	Gums and Mucilage	-

+++: highly present, ++: moderately present, +: Low; (+) < (++) < (+++): Based on the intensity of the characteristics colour observed.

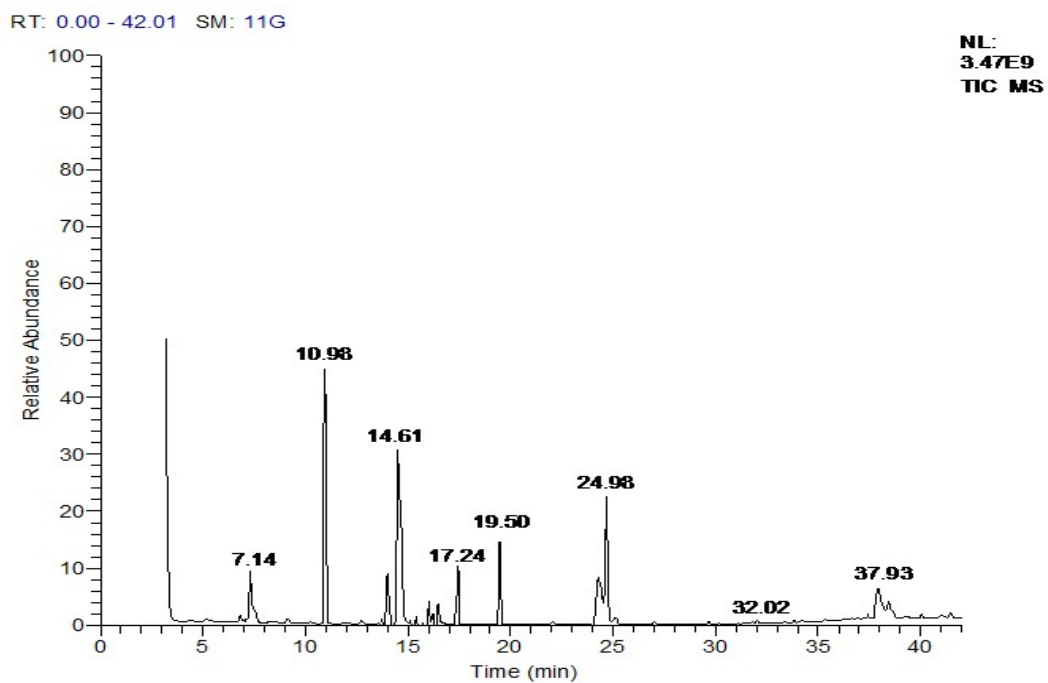


Fig. S1. GC-MS analysis chromatogram of *K. laciniata* methanolic extract

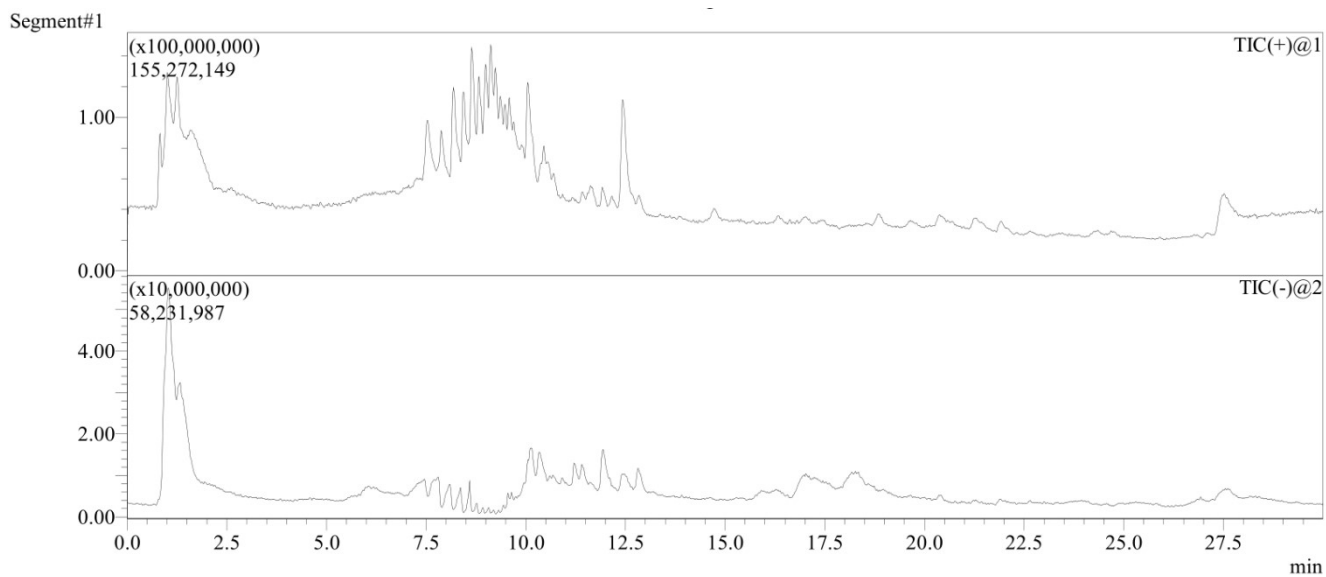


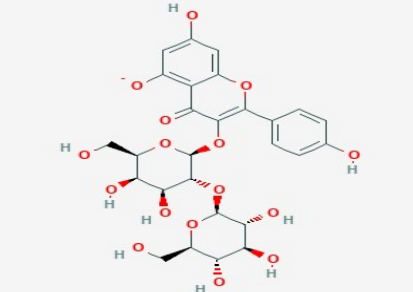
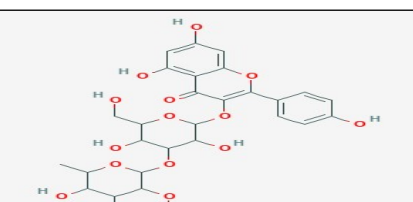
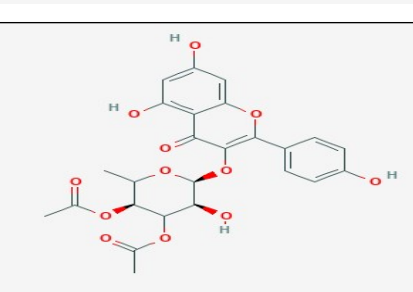
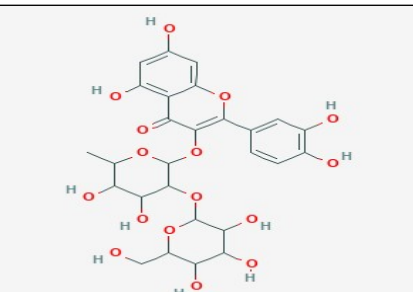
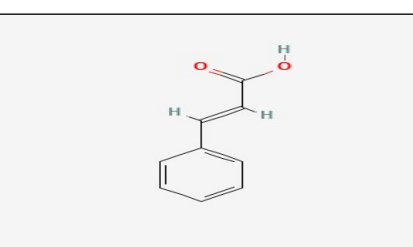
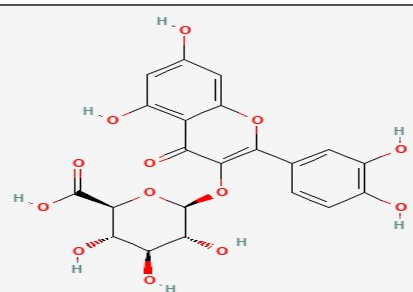
Fig. S2. LC-MS analysis chromatogram of *K. laciniata* methanolic extract

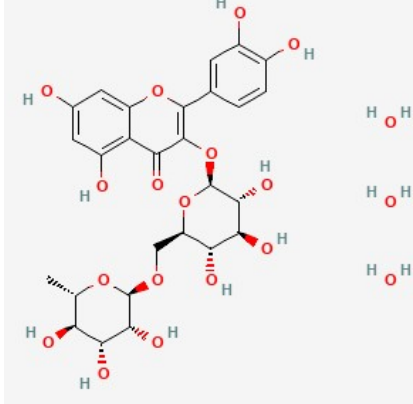
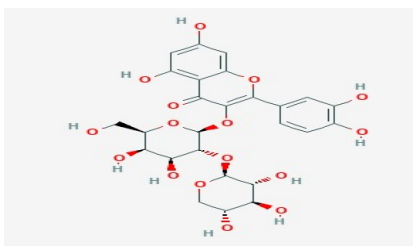
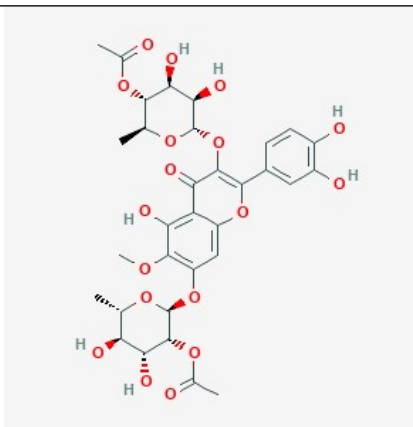
Table. S2. Characteristics of compound

Characteristics of selected bioactive compounds identified from *Kalanchoe laciniata* and shortlisted from the compound–target interaction network. The table summarizes the compound name, molecular formula, two-dimensional (2D) chemical structure, and predicted network pharmacology parameters including closeness centrality (CC), betweenness

centrality (BC), and average shortest path length (ASPL), derived from the compound–target network analysis. These metrics reflect the relative importance and connectivity of each compound within the interaction network and were used to prioritize key compounds for further in silico evaluation.

Compound Name	Molecular formula	2D Structure	CC	BC	ASPL
Kalanchoside C	C₃₀H₄₂O₉		0.39	0.14	2.54
Kalanchoside B	C₃₀H₄₂O₁₀		0.39	0.14	2.54
Oleanolic acid beta-D- glucopyranosyl ester	C₃₆H₅₈O₈		0.39	0.20	2.54
Patuletin	C₁₆H₁₂O₈		0.39	0.09	2.54
Stigmasterol	C₂₉H₄₈O		0.39	0.23	2.54

kaempferol 3-O- (2'-O-D- glucopyranosyl)- beta-D- galactopyranoside	<u>C₂₇H₂₉O₁₆</u>		0.39	0.039	2.54
Kaempferol-3-O- glucoside-3"- rhamnoside	<u>C₂₇H₃₀O₁₅</u>		0.39	0.04	2.54
Kaempferol 3- (3",4"- diacetyl rhamnosi- de)	<u>C₂₅H₂₄O₁₂</u>		0.39	0.13	2.54
Quercetin 3-(2- glucosyl rhamnosi- de)	<u>C₂₇H₃₀O₁₆</u>		0.39	0.044	2.54
Cinnamic acid	<u>C₉H₈O₂</u>		0.39	0.17	2.54
Miquelianin	<u>C₂₁H₁₈O₁₃</u>		0.39	0.04	2.54

Rutin trihydrate	<u>C₂₇H₃₆O₁₉</u>		0.39	0.035	2.54
Quercetin 3-O- .beta.-D- xylopyranosyl-(1- ->2)-.beta.-D- galactopyranoside	<u>C₂₆H₂₈O₁₆</u>		0.390	0.044	2.54
Kalambroside-A	<u>C₃₂H₃₆O₁₈</u>		2.54	0.17	0.39

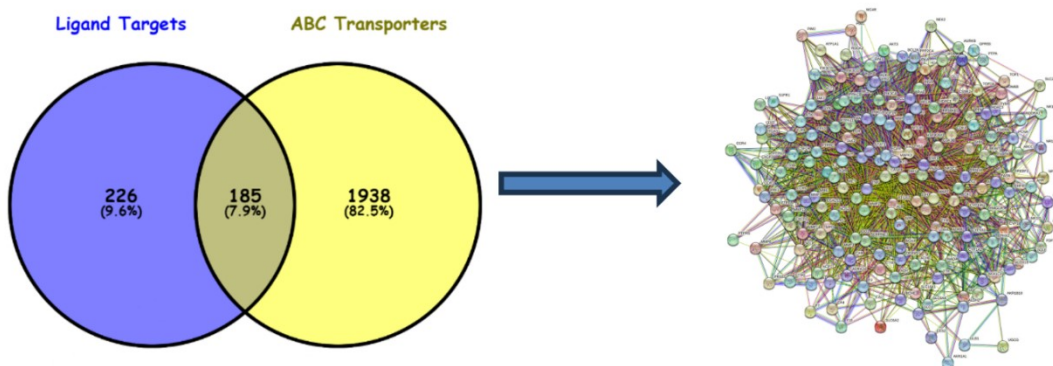


Fig. S3. Common genes String analysis displayed along with Venn diagram of ligand targets and ABC transporters, used to identify common genes.

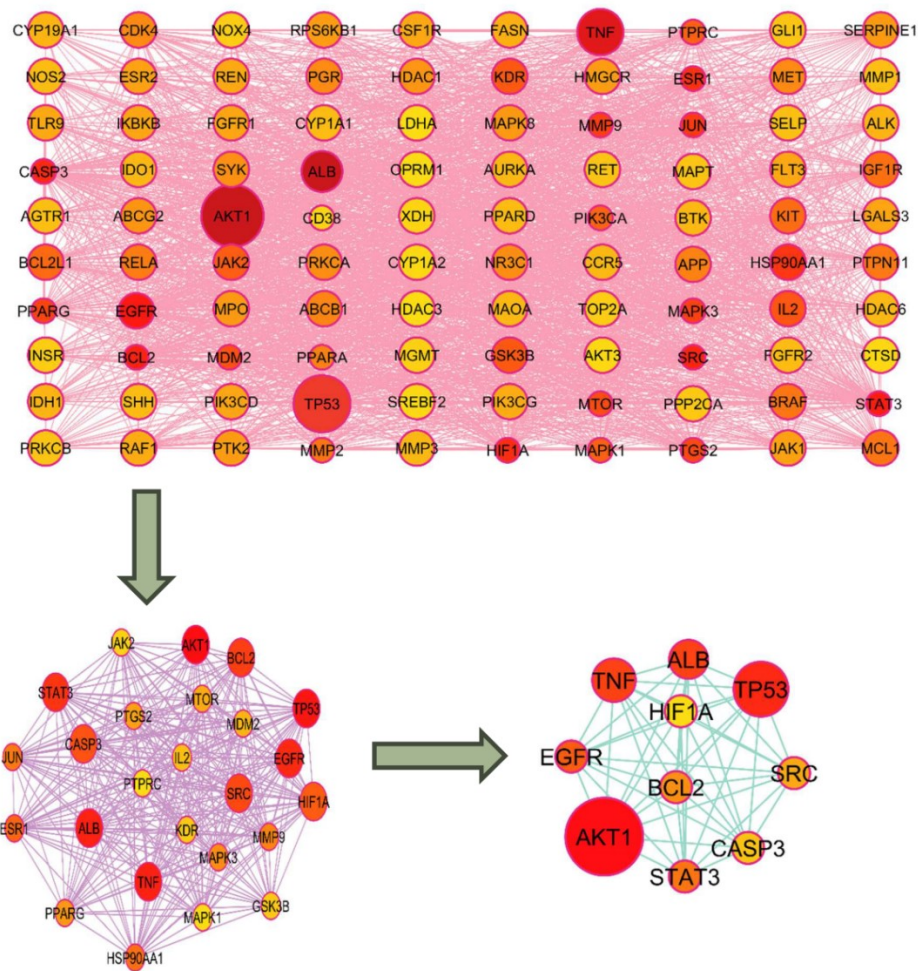


Fig. S4. Protein-protein interaction network of Top 100 common targets of *K. laciniata* and ABC transporters the larger the node indicates the dark colour, the larger its degree value in the network, and the greater its importance within the network.

Table S3. Network Topology of ABC Transporter-Associated Targets Modulated by KLM

Target Name	Degree	CC	BC	ASPL
AKT1	119	0.045	0.73	1.35
TP53	116	0.040	0.72	1.37
TNF	113	0.051	0.72	1.38
ALB	113	0.076	0.72	1.38
EGFR	111	0.044	0.71	1.40

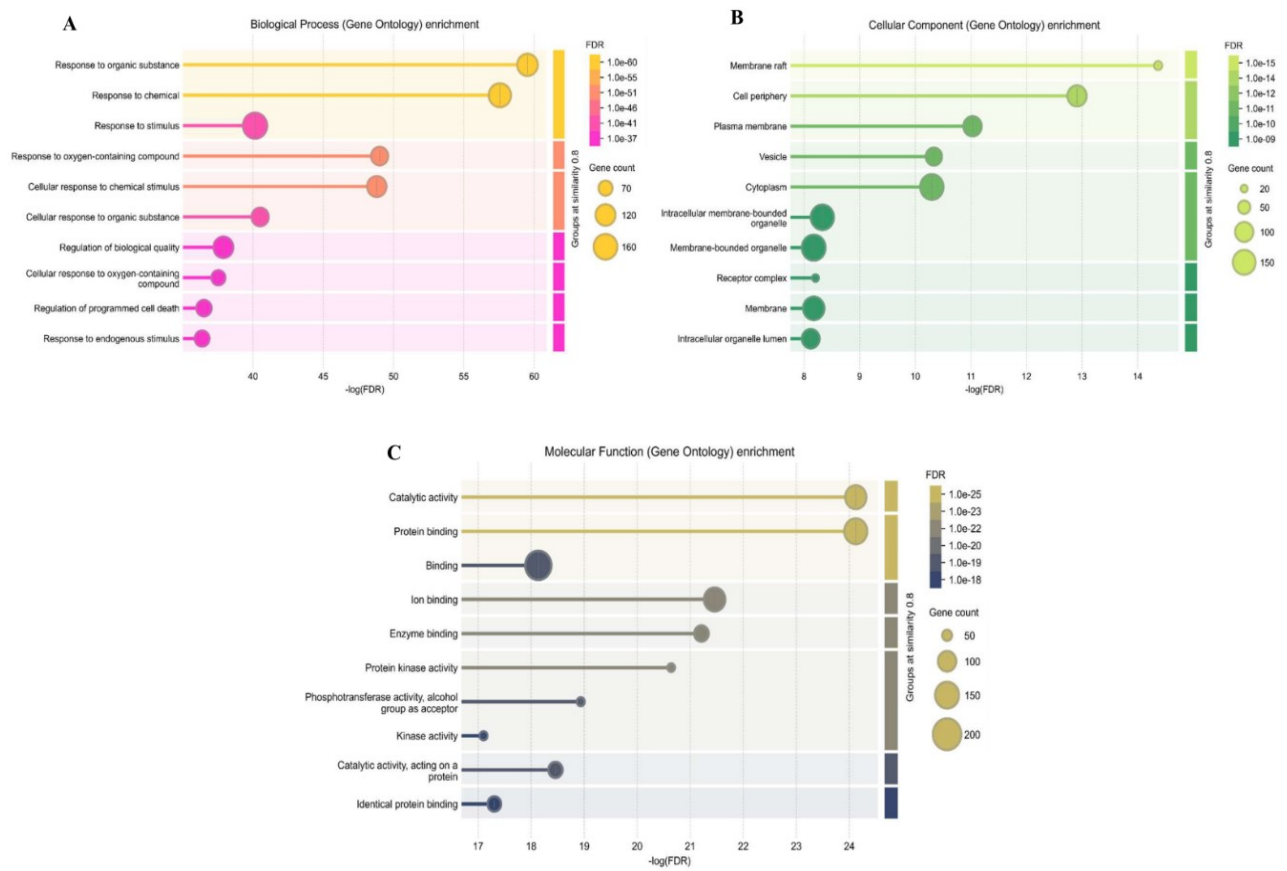


Fig. S5(A-C). **A.** shows the Biological Processes enriched, **B** shows the cellular components enriched, and **C** shows the Molecular Functions enriched by the common genes.

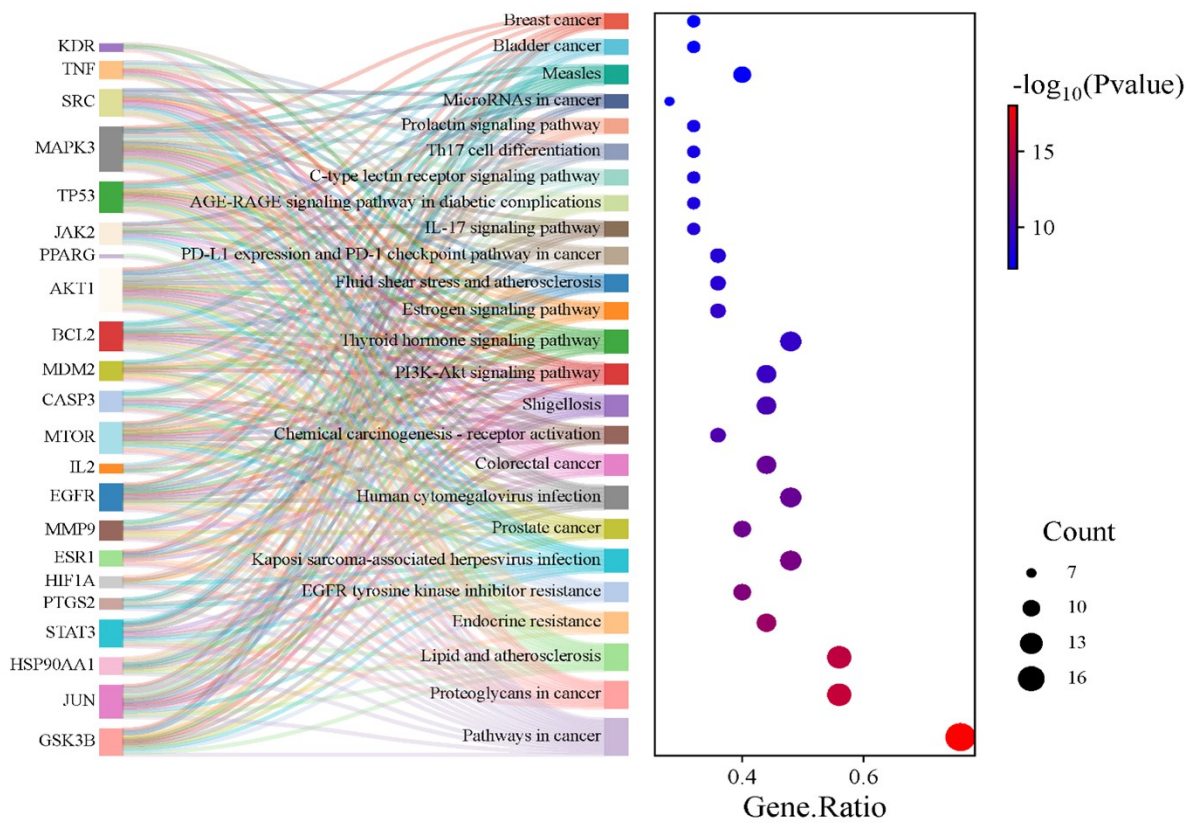


Fig S6. Bubble graph of top 20 signalling pathways

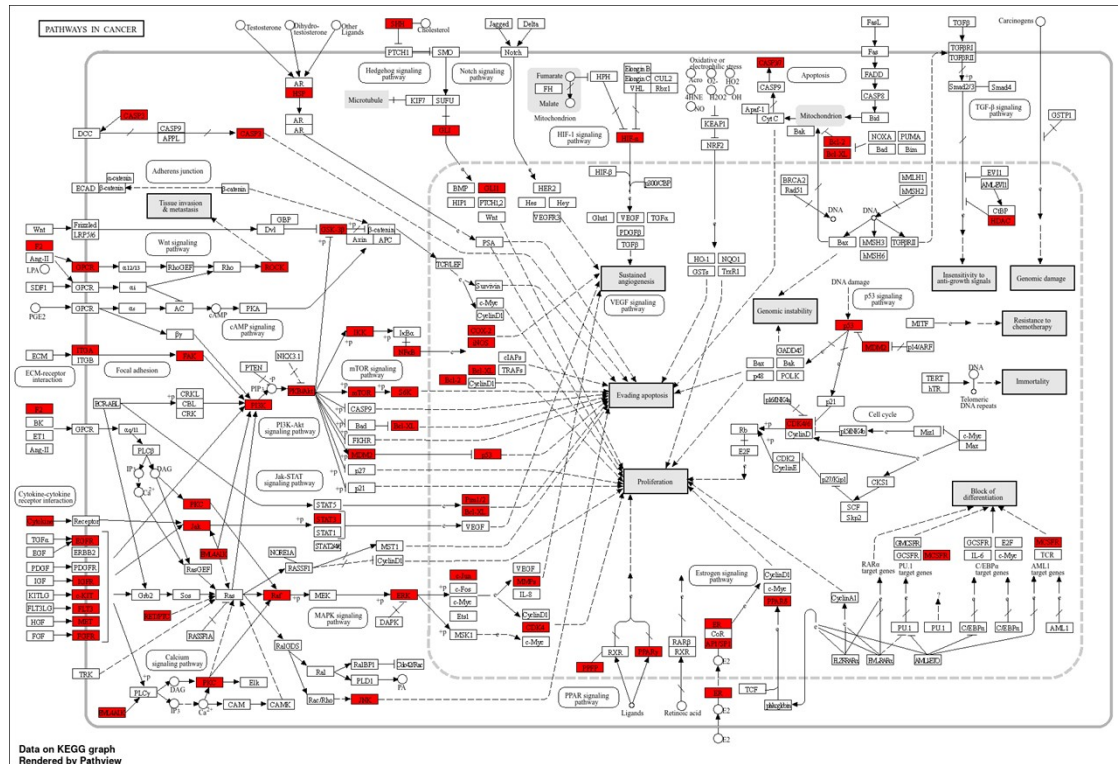


Fig S7. KEGG graph of common genes involved in different pathways in cancer.

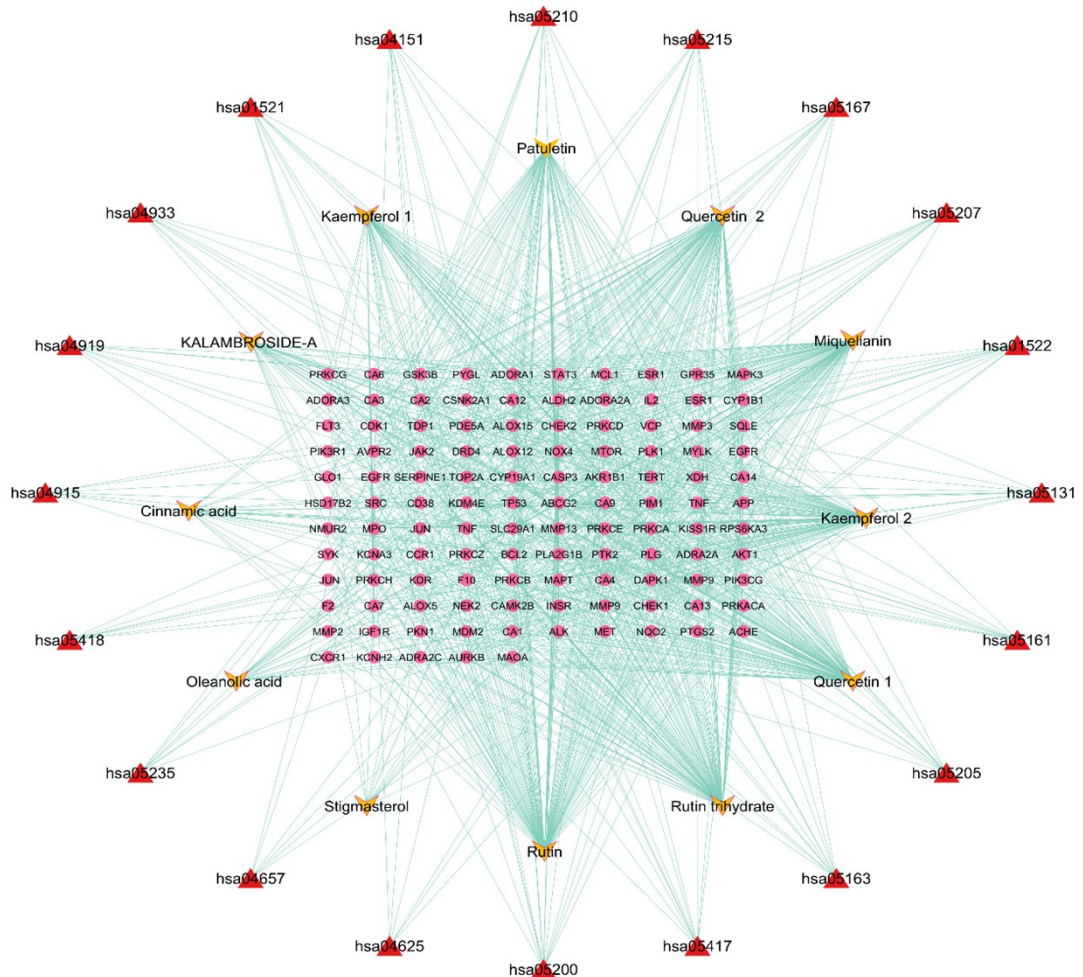


Fig. S8. Visualization of active compounds–potential targets–signalling pathways. Red node represents the signalling pathways; yellow node represents the active compounds and pink node represents the potential targets. Where hsa05200:Pathways in cancer, hsa05205:Proteoglycans in cancer, hsa05417:Lipid and atherosclerosis, hsa01522:Endocrine resistance, hsa01521:EGFR tyrosine kinase inhibitor resistance, hsa05167:Kaposi sarcoma-associated herpesvirus infection, hsa05215:Prostate cancer, hsa05163:Human cytomegalovirus infection, hsa05161:Hepatitis B, hsa05210:Colorectal cancer, hsa05207:Chemical carcinogenesis - receptor activation, hsa05131:Shigellosis, hsa04151:PI3K-Akt signalling pathway, hsa04919:Thyroid hormone signalling pathway, hsa04915:Estrogen signalling pathway, hsa05418:Fluid shear stress and atherosclerosis, hsa05235:PD-L1 expression and PD-1 checkpoint pathway in cancer, hsa04657:IL-17 signalling pathway, hsa04933:AGE-RAGE signalling pathway in diabetic complications, hsa04625:C-type lectin receptor signalling pathway.

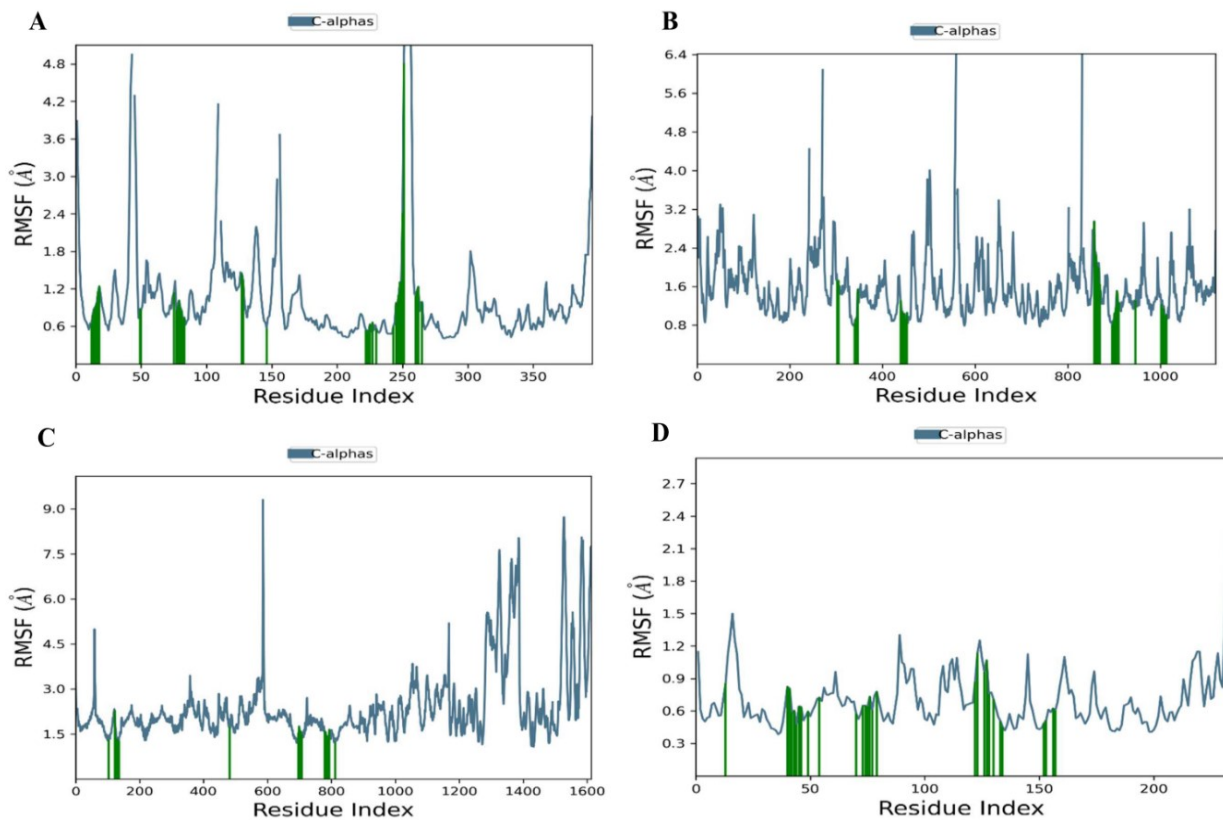


Fig. S9 (A-C) RMSF plot of different protein-ligand complexes. (A - AKT1 & Quercetin 3-O-beta-D-xylopyranosyl-(1--2)-beta-D-galactopyranoside), (B - BCRP & Rutin), (C - P-gp & Quercetin 3-O-beta-D-xylopyranosyl-(1--2)-beta-D-galactopyranoside), and (D - MRP1 & Quercetin 3-(2-glucosylrhamnoside))

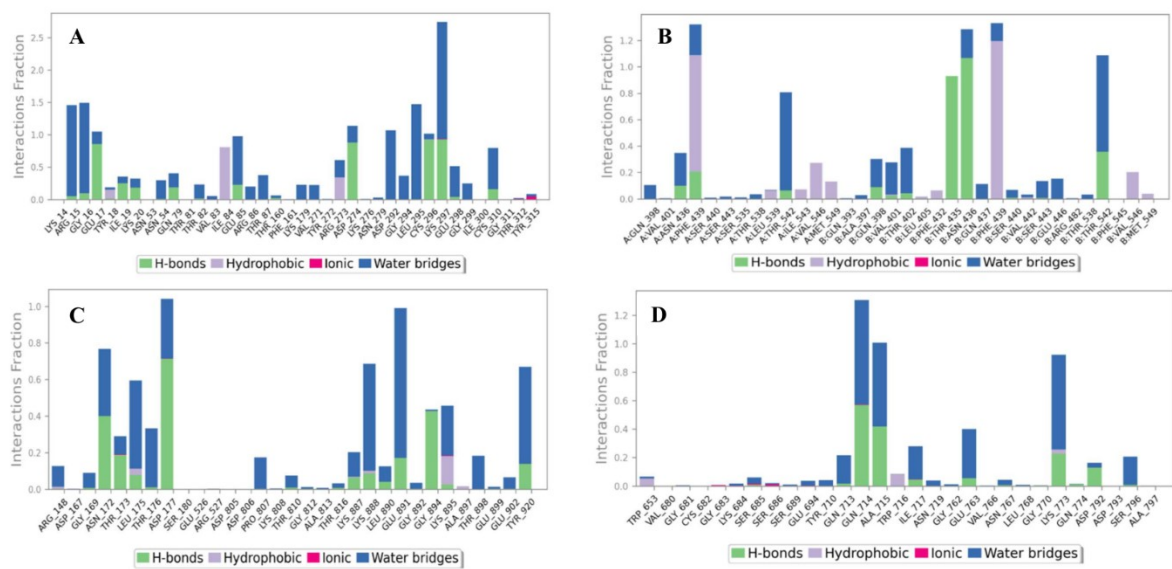


Fig. S10 (A-C) Protein-Ligand contact types all four protein-ligand complexes. (A - AKT1 & Quercetin 3-O-beta-D-xylopyranosyl-(1--2)-beta-D-galactopyranoside), (B - BCRP & Rutin), (C - P-gp & Quercetin 3-O-beta-D-xylopyranosyl-(1--2)-beta-D-galactopyranoside), and (D - MRP1 & Quercetin 3-(2-glucosylrhamnoside))

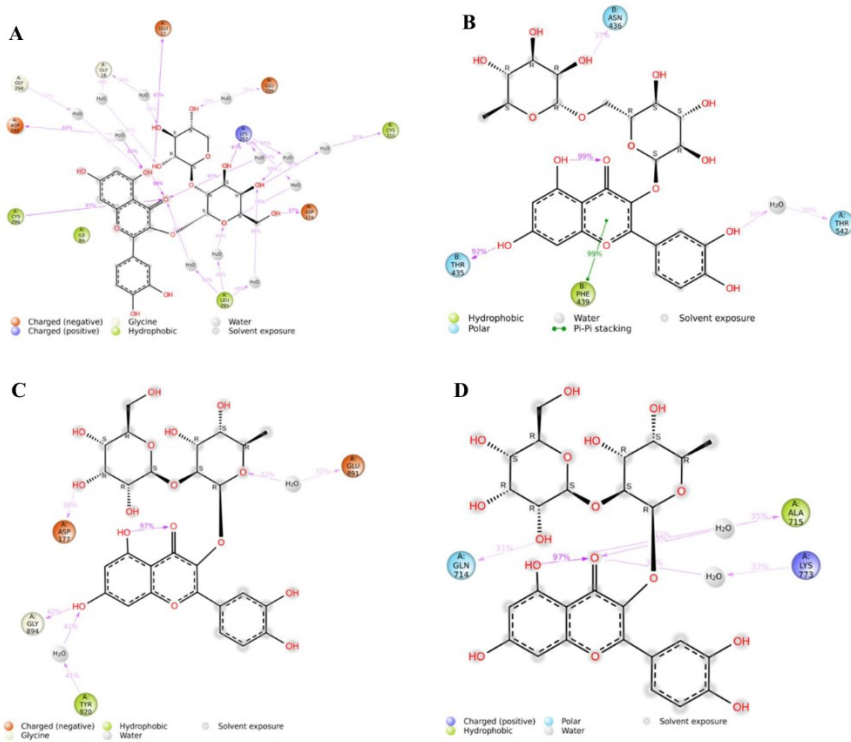


Fig. S11 (A-D) 2D protein-ligand interaction diagrams of different protein-ligand complexes. (A - AKT1 & Quercetin 3-O-beta-D-xylopyranosyl-(1--2)-beta-D-galactopyranoside), (B - BCRP & Rutin), (C - P-gp & Quercetin 3-O-beta-D-xylopyranosyl-(1--2)-beta-D-galactopyranoside), and (D - MRP1 & Quercetin 3-(2-glucosylrhamnoside)).

Effects of *Kalanchoe laciniata* extract on the viability of the RIN-5F cell line

The cytotoxic potential of the methanolic leaf extract of *Kalanchoe laciniata* (KLM) was assessed in normal pancreatic β -cell line RIN-5F using the MTT assay to evaluate its selectivity toward cancer cells. Cells were exposed to varying concentrations of the extract ($100\text{--}600 \mu\text{g mL}^{-1}$) for 24 hours, and cell viability was determined spectrophotometrically. The results revealed a concentration-dependent reduction in cell viability, with percentage inhibitions of 37.43%, 39.97%, 61.15%, 66.32%, and 87.98% at 100, 200, 300, 500, and 600 $\mu\text{g mL}^{-1}$, respectively. The IC_{50} value of the extract against RIN-5F cells was calculated to be 242.17 $\mu\text{g mL}^{-1}$, indicating moderate cytotoxicity in normal cells. When compared to the IC_{50} value obtained for MDA-MB-231 breast cancer cells ($60.55 \mu\text{g mL}^{-1}$), the substantially higher IC_{50} in RIN-5F cells suggests a favorable degree of selectivity and safety of the extract toward normal cells. While RIN-5F cells were used to assess non-specific cytotoxicity, future investigations incorporating normal mammary epithelial models such as MCF-10A will be necessary to confirm breast tissue-specific selectivity.

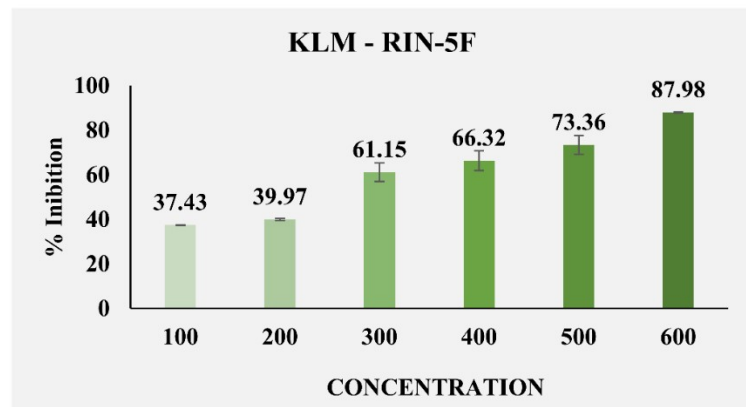
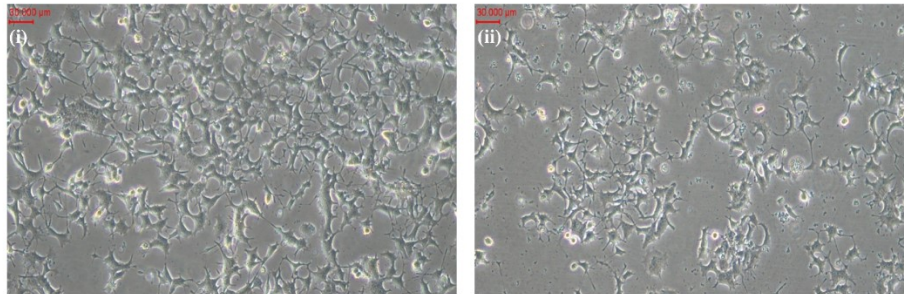
A**B**

Fig. S12 (A-C). **A.** Determination of cytotoxicity of *Kalanchoe laciniata* methanolic extract (KLM) on normal RIN-5F cells (% inhibition of cell growth) by MTT assay. RIN-5F cells were treated with varying concentrations of the KLM extract ($100\text{--}600 \mu\text{g/mL}^{-1}$) for 24 hours. Data are presented as mean \pm standard deviation (SD) of triplicate experiments, with error bars representing variability among replicates. Statistical significance was evaluated using one-way analysis of variance (ANOVA). **B.** Morphological examination of RIN-5F cells following treatment with *Kalanchoe laciniata* methanolic extract (KLM) assess cell proliferation inhibition. (I) untreated cells under optical microscope showing excellent cell density (II) KLM treated cells with a marked reduction in viable cells.